VARIATION OF THE APPARENT DIFFUSION COEFFICIENT OF SKULL BONE MARROW WITH AGE, PUBERTAL STATUS AND GENDER IN A PAEDIATRIC POPULATION

Erika Pace[a, b] MD, MRCR

Andrew D MacKinnon[b, c] MD, MRCP, FRCR

Nandita M deSouza[a, b] MD, FRCR

1 CRUK Imaging Centre, The Institute of Cancer Research, Sutton, UK

2 The Royal Marsden Hospital, Department of Radiology, Sutton, UK

3 Department of Neuroradiology, Atkinson Morley Regional Neuroscience Centre, St George's University Hospitals NHS Foundation Trust, London, UK

Author for correspondence:
Nandita M deSouza
The Institute of Cancer Research and The Royal Marsden Hospital
Downs Road
Sutton
Surrey SM2 5PT
United Kingdom
Telephone: +44-8661-3289
Email: nandita.desouza@icr.ac.uk

Funding acknowledgements:
CRUK and EPSRC support to the Cancer Imaging Centre at ICR and RMH in association with MRC and Department of Health C1060/A10334, C1060/A16464 and NHS funding to the NIHR Biomedical Research Centre and the Clinical Research Facility in Imaging.

Declaration of Conflicting Interests:
All authors and author institutions have no conflicts of interest.

We can confirm the article is not under consideration for publication elsewhere. Each author takes full responsibility for its content. Publication has been approved by all authors.

Abstract

Background

Bone marrow composition varies with stage of development.

Purpose

To assess differences in apparent diffusion coefficient (ADC) derived from clivus bone marrow in healthy children by age, pubertal status and gender as a benchmark when monitoring local and systemic treatment-induced effects.

Materials and Methods

Non-oncological paediatric subjects (30 pre-pubertal [15 female, 15 male] and 30 post-pubertal [15 female, 15 male]) with previous normal MRI-Brain including Diffusion Weighted Imaging (1.5T Philips Achieva-Ingenia, b-values 0 and 1000s/mm^2) were studied. A 4-6mm diameter region-of-interest (ROI), drawn within the clivus on two or three diffusion-weighted image slices, yielded mean and centile ADC values. Pubertal status was recognised from imaging appearances of the pituitary gland and from fusion of the spheno-occipital synchondrosis. Correlations between ADC and age were assessed (Pearson's coefficient). Mann-Whitney-U tests compared ADC by age, pubertal status and gender.

Results

Age and ADC were significantly negatively correlated (median ADC r=-0.48 mean ADC r=-0.42, p=0.0001 and 0.0008 respectively) which held true when divided by gender. Mean and median ADC differed significantly before and after puberty for the whole population (p=0.0001 and 0.0001 respectively). There was a left shift of the ADC histogram post-puberty with significant differences in centile values. ADC differences pre- and post-puberty

remained when divided by gender (females p=0.04 and 0.009 respectively; males p=0.005 and 0.0002 respectively).

Conclusion

ADC of clivus bone marrow correlates with age in children. ADC decreases significantly post-puberty, likely due to replacement of hypercellular marrow with fat. There are no gender-related differences in ADC pre- or post-puberty.

Keywords

Diffusion-weighted MRI; apparent diffusion coefficient; bone marrow; puberty; gender; paediatric

Introduction

Bone marrow composition varies with biological and physiological requirements at different stages of development (1). Haematopoietic cells appear within the medullary cavities of bones at around 14 weeks of gestation (2). By birth the bone marrow represents the principal anatomical location of haematopoiesis. The marrow space occupied by haematopoietic cells diminishes from 90% at birth to approximately 50% at 30 years old and 30% at age 70 as it becomes progressively replaced by fat (3, 4). The relative proportion of marrow haematopoietic vs. fat components also classically depends on the type of bone (long, short, flat and irregular). Until puberty the entire skeleton remains haematopoietically active, but by age 18 the production of blood cells persists only in the vertebrae, ribs, sternum, skull, pelvis, proximal humeral and femoral epiphyses, whilst other osseous locations bones undergo fatty infiltration (5). An indication of the proportion of cellular vs. fatty component of the bone marrow in children would be informative on the proliferative state of the bone marrow and on changes that occur as a result of therapy.

Diffusion-weighted MRI uses non-ionizing radiation without administration of extrinsic contrast agents to characterise tissues. Its quantified metric, the apparent diffusion coefficient (ADC), has been strongly linked to cell density of tissues (6). Moreover, the sequence uses a fat suppression pulse, so that fat interspersed within tissue results in a reduction in ADC. Although there is no direct quantification of fat, lower ADC values have been used as a surrogate for the appearance of fat within bone marrow of the axial and appendicular skeleton in several studies in adults (7, 8). There is limited data on ADC values in normal, healthy children (9), but no studies to date have documented differences in cellular vs. fat components of bone marrow in children by age, pubertal status and gender.

This work retrospectively studied bone marrow in the skull because DW-MRI forms a routine part of brain imaging in children. The flat shape of the skull bones meant that region-of-interest (ROI) delineation in the skull was best done in the clivus. This area of the skull base represents one of thickest bones within the cranium, making ROI in multiple adjacent slices with an interval of 5 mm feasible. Additionally, its midline location means that the clivus is routinely included in the field of irradiation as a treatment for brain tumour, making it ideally placed for measurement of treatment-related ADC changes in future studies. The purpose of this study, therefore, was to assess the differences in ADC derived from the bone marrow of the clivus in a healthy paediatric population by age, pubertal status and gender.

Methods

Patient Selection

Non-oncological paediatric subjects who previously had brain MRI for clinical purposes and in whom DWI was routinely performed as part of the examination were studied. The study was approved by the Institutional Review Board and the need for written consent was waived.

Inclusion and exclusion criteria chosen were to allow the retrospective selection of a cohort of paediatric patients (5-17 years old) with normal MRI brain scans (n=60) with diffusion-weighted imaging that was artefact-free. Electronic Patient Records were assessed to confirm clinical presentation and any follow up diagnosis. Indications for MRI were headaches, transient neurological symptoms, syncopal episodes and possible seizures (but with normal electroencephalogram). Patients with any condition that might affect the bone marrow (infection, bone lesions at any site, systemic diseases, oncological diagnosis or on medication) were excluded. Of 1,140 children identified on the database over a 2-year period (1st March 2016-31st March 2018), 60 individuals met these stringent exclusion criteria all of whom were included in the analysis.

Image acquisition

All children had been scanned on a 1.5 T Philips Achieva-Ingenia upgraded to d-stream (digital rf) platform. Their examinations were anonymized and transferred to a research imaging repository at The Institute of Cancer Research through a secure web-based data analysis platform. Axial single-shot echo-planar diffusion-weighted images (b-values = 0 and 1000 s/mm^2) were routinely acquired as part of the standard MRI brain scan. The voxel

resolution was 0.9375 x 0.9375 x 4 mm. Axial T2-W spin-echo (SE) and Fluid-Attenuated Inversion Recovery (FLAIR), as well as sagittal T1-W SE and coronal T2-W SE images were acquired in each case. In individuals older than 16 years, the sagittal T1-W SE was replaced by T2-W SE. These images were part of a standard anatomical protocol for brain imaging and were not optimised for bone marrow study; they were not utilised in this study.

Image Analysis

T2-weighted images were used to identify the exact location of the clivus. The axial DW images were then correlated with morphological T2-weighted images. A circular region-of-interest (ROI) of 4-6 mm in diameter was drawn within the clivus on the diffusion-weighted images (EP, paediatric radiologist, 2 years' experience) using in-house software (Adept®, The Institute of Cancer Research, UK). Care was taken to include the maximum number of pixels from clival marrow whilst avoiding contamination from surrounding bony cortex (**Figure 1**). In n=58 cases this was possible on 2 central slices; in 2 cases, ROIs were possible in 3 adjacent slices. To avoid including artefacts, the ROIs were drawn within the clivus at the level of the fossa navicularis. Use of the high b-value image for ROI definition rather than the ADC map ensured reliable placement within the high-signal of clivus marrow. Each patient measurement to review images, plan ROI placement and extract and tabulate the ADC values took ~15 mins. To determine interobserver variability of the measurement, a second observer (NdS, MR radiologist 25 years' experience, non-specialist in paediatric neuroradiology) independently drew an ROI within the clivus on a single central slice of the diffusion-weighted images in a randomly selected subset of 20 subjects (5 from each group). Data from the entire volume of the ROIs were extracted and the ADC calculated on a voxel-by voxel basis using a monoexponential fit of the data. This yielded a range of ADC values

for each subject from which median, mean, 10^{th}, 25^{th}, 75^{th} and 90^{th} percentiles were derived. Traditional ADC maps were also created.

Recognition of pubertal status was radiological in the 10-17-year-old age group. Puberty was determined from the imaging appearances of the anterior pituitary gland (convex bulging above the sella superiorly) together with spheno-occipital synchondrosis fusion (**Figure 1**). At puberty there is physiological enlargement of the anterior pituitary gland, often more notable in females, when the gland develops a convex superior border and often bulges just out of the sella. The appearance of the anterior pituitary gland was assessed on both sagittal (T1-weighted images if younger than 16 years and T2 if older as per adult MR routine protocol) and coronal T2-weighted images (10). In addition, the maturation stage of spheno-occipital synchondrosis closure was assessed on the sagittal MRI images (**Table 1**). Its relationship to puberty has been described in a recent study and proposed on CT. Stages 0 and 1 were considered pre-pubertal and stages 2 and 3 post-pubertal (11).

Data Analysis

Statistical analysis was performed using Excel and GraphPad Prism software (version 7.04, GraphPad Incorporated company, California). Descriptive statistics were used to describe the data. Data was checked for normality (D'Agostino and Pearson normality test); although the data from female subjects was normally distributed, that from males was not. Therefore, a Mann-Whitney U test was used to compare groups. A Pearson's correlation coefficient examined the relationship between ADC and age.

Results

Of 60 children who met the selection criteria there were 15 aged 5-9 years (8 female, 7 male), 15 pre-pubertal aged 10 years and older (7 female, 8 male), 15 post-pubertal females and 15 post-pubertal males.

The number of voxels included in each case ranged from 21 to 182 and was significantly different among the groups (5-9 years, mean ± std = 78.8 ± 30.8; pre-pubertal aged 10 years and older, mean ± std = 57.1 ± 12.4; post-pubertal females, mean ± std = 40.5 ± 7.2; post-pubertal males, mean ± std = 39.5 ± 14.7; $p < 0.0001$).

Interobserver variability (95% limits of agreement) ranged from -11 to +13% for median ADC values and -13 to +14% for mean ADC values (**Figure 2)**.

Variation with age

Age ranged from 5.0 to 17.9 years (median 12.4 years). There was a significant negative correlation between age and ADC for the whole cohort ($r = -0.48$ for median and -0.42 for mean values, $p = 0.0001$ and 0.0008 respectively). There was also a significant negative correlation between age and ADC for females ($r = -0.5$ for median and -0.4 for mean values, $p = 0.005$ and 0.03 respectively) and for males ($r = -0.53$ for median and -0.48 for mean values, $p = 0.002$ and 0.008 respectively). Regression plots for median values are illustrated in **Figure 3**.

Variation with pubertal status

Age of the pubertal cohort ranged from 12.3 to 17.9 years; it was lower in females (median age 15.1 years, range 12.3 to 17.9 years), compared to males (median age 16.8 years, range 13.7 to 17.8 years).

There was a significant difference between mean and median ADC values before and after puberty for the whole population (**Table 2, Figure 4**), which was greater than the 95% limits of agreement for interobserver variability. There was a shift of the ADC histogram to the left post-puberty (**Figure 5a**) as evidenced by the significant difference in centile values across the population. This is illustrated in exemplar cases pre- (**Figure 6**) and post- (**Figure 7**) puberty. However, this was not reflected in an increased homogeneity of values as the interquartile range did not change (**Table 2**).

Variation with gender

Pre-puberty, there were no significant differences in mean or median ADC in females vs. males ($p= 0.3$ for mean, 0.1 for median and >0.05 at all centile values).

The pre- and post-puberty differences seen for the whole cohort also held true for females alone and males alone (**Table 3, Figure 4**) with striking reductions in mean and median ADC and a left shift of histogram centile values (**Figure 5b and c**). Differences between the whole cohort comparison pre- and post-puberty and the same comparison done by gender (females alone and males alone) were evident, for example the lack of significance between the 90^{th} centile values for females and the 10th centile values for males. However, these differences are likely to relate to the smaller patient numbers when divided by gender rather than representing true differences.

Discussion

This is a first report of variation in ADC values in bone marrow with age, pubertal status and gender in a healthy paediatric population. A large study of 500 subjects in 7 groups had the 6-14 year age group categorised as one, and did not interrogate the effects of puberty on the bone marrow (12). Whilst many reports exist linking sex hormones to cortical bone mass at puberty in both preclinical (13, 14) and clinical (15, 16) studies, there is a paucity of data on how the onset of puberty results in measurable changes within the marrow itself. This has been limited by the previous means of studying bone marrow, which required invasive biopsy and did not interrogate the entire skeleton. The advent of quantitative MRI biomarkers has changed the landscape in this regard (17, 18) and makes it possible to prospectively derive measurements from bone marrow both within a region or at a whole skeleton level (using whole-body MRI) in order to study changes with normal physiology and with treatment (19).

We report a significant correlation of ADC with age. A recent publication reporting data in the lumbar spine did not indicate such a change with age as children matured (9). Their mean and median ADC values remained between 0.58 and 0.63 x 10^{-3} mm^2/s across all age groups. However, their data did not separate individuals by pubertal status and the distribution of children vs. young adults in their cohort is likely to have represented individuals who were chiefly post-pubertal.

It is well established that cancellous bone decreases and bone marrow fat content increases with age. This physiological replacement of haematopoietic cells with adipocytes correlates directly with age (20), reaching a peak in young adults. Marrow adiposity has been inversely related to cortical bone area in young adults (21) and to bone mineral content (12). However, this step-change at puberty has not been recognised. Although there is extensive evidence

linking fat replacement in the marrow of adults to steroid therapy, there is no data linking the increase in marrow fat to the surge of sex steroid hormones at puberty. A recent study in a preclinical mouse model has elegantly demonstrated that leutinizing hormone is involved in haematopoietic stem cell homeostasis (22); it may well be that the expression of this receptor particularly at sites within long bones and where haematopoietic function is no longer needed post-puberty is one molecular mechanism driving the replacement of this functionally active tissue with fat.

The factors governing the relative amounts of haematopoietic and fatty components was elegantly hypothesized by Gurevitch (23) where a dependence on the number of pluripotent mesenchymal stem cells (that differentiate to support both osteogenesis and haematopoiesis) was recognized. They hypothesized that as these cells are bound to endosteal and trabecular surfaces, they were numerous in growing tubular and cancellous bone, but once maturity was reached, they were far less numerous in tubular bones than in cancellous bone, because of the smaller internal bone surface area in the former. Post-maturity, therefore, mesenchymal stem cells in tubular bones favour support of a critical osteogenic function while in cancellous bone where they are more numerous, they retain a hematopoietic support function because of continued direct contact with hematopoietic cells. In the absence of hematopoietic cells they change into fat-accumulating cells (24) so that fat-fraction increases. T1 measurements have been used to estimate fat fraction (25). Although this was not possible in this retrospective study, it would be of interest to quantify regional bone marrow fat changes in the skeleton with the onset of puberty.

The relationship between bone marrow cellularity and ADC was established more than a decade ago, where a study that correlated cellularity in ilium aspirate was correlated with ADC values in 37 adults and children (26). The 5 young children in Nomomura's study did

not have bone marrow aspirate performed, but their marrow was considered hypercellular in view of their age (0-3 years). Unfortunately, the b-values used in this study were low (0 and 350 s/mm^2), so are likely to represent perfusional effects rather than true diffusion. This is reflected in the relatively high absolute values of 0.827 and 0.708 x 10^{-3} for normocellular marrow in the adults in their cohort. Unfortunately, also, the absolute cellularity of the aspirates was not quantified, so the relationship between the ADC and cellular "burden" has not been established.

Determining a ROI in flat-bones of a paediatric skull is challenging. Using the clivus ensured that a 4-6 mm diameter circular ROI could be obtained on 2 or 3 slices so that at least 21 voxels could be included in each scan. In future, automated segmentation methods may well enable more accurate delineation of the entire skull, which would enable larger scale analyses of this type. A previous extensive study in 500 subjects, 200 of whom were under 14 years old (27) examined the differences in ADC values by skull location and correlated values with age. Interestingly the occipital and parietal bones showed a variation with age, with a gradual downward trend between 0 and 30 years, whereas the frontal and temporal bones did not. This is in keeping with the findings in our study where the clivus as part of the occipital bone at the skull base shows this change. It indicates that, as with the tubular bones, the haemopoietic function of the skull base becomes less important with age, while that of the frontal and temporal regions is unaltered into adult life (27).

Signal-to-noise ratio is critically important in the reliability of the ADC measurement. ROIs within the clivus allowed inclusion of at least 21 voxels and had the advantage of avoiding sutures with a homogenous area from which to derive quantitative data. Other studies of bone marrow in children have focused on larger areas afforded by the vertebrae and iliac bones (9). Nevertheless, the values we obtained here are in keeping with those from these other studies.

Our study had several limitations. Firstly, it was retrospective and relied on selecting healthy children with normal MRI brain scans. We attempted to mitigate against errors from inclusion of likely pathologies or treatment related effects by having very strict inclusion and exclusion criteria. We interrogated a large pool of >1000 children scanned over a 2-year period to derive these patient numbers for investigation. In future, exploiting data from image biobanks may be possible. Secondly, only 2 b-values were used in the acquisition for derivation of ADC and one of them was b=0. It is now established that elimination of perfusional effects to obtain a true D* necessitates the lower b-value is >50 mm^2/s (28). A third b-value between 50 mm^2/s and 1000 mm^2/s ensures robustness of the ADC calculation. Although this was not available, our quantified values were similar to other cited literature values (29). Thirdly, we did not directly measure fat-fraction, although this report assumes the relationship between ADC and fat fraction is inverse, so explaining our findings (7). Fourthly, our assessment of puberty, although objective and done on imaging grounds was not confirmed by blood hormone profiles in these children. Although a prospective longitudinal study pre- and post-puberty as verified by hormone profiles is the ideal, this is difficult to justify. It would, however, establish definitively whether there was a linear correlation of ADC with age or a step-change at puberty. Our data shows a negative correlation of ADC with age and illustrates the range of normal values, but the sample size is too small to differentiate a linear decrease of ADC with age from a step-change at puberty. Finally, measuring ADC reproducibility would have been ideal, but as our cohort were children with minimal symptoms, a second/follow-up MRI scan was not justified. Measurement of ADC in adult populations has indicated that it is a robust measurement in normal bone marrow (30), and that the differences reported in this study are greater than the published limits of agreement.

In conclusion, this study shows a correlation of ADC with age in children. Moreover, it is the first study to document a significant change in marrow ADC related to puberty, using the ADC of marrow in the clivus as a quantitative biomarker. There were no discernible differences by gender. These data will form the basis for understanding changes that occur in the bone marrow following local and systemic treatments of haematological and non-haematological malignancies.

Acknowledgements

BLINDED

Declaration of Conflicting Interests

All authors and author institutions have no conflicts of interest.

REFERENCES

1. Proytcheva M**.** Bone marrow evaluation for pediatric patients. Int J Lab Hematol 2013:283-9.
2. Chen LT, Weiss L**.** The development of vertebral bone marrow of human fetuses. Blood 1975:389-408.
3. Blebea JS, Houseni M, Torigian DA, et al. Structural and functional imaging of normal bone marrow and evaluation of its age-related changes. Semin Nucl Med 2007:185-94.
4. Malkiewicz A, Dziedzic M**.** Bone marrow reconversion - imaging of physiological changes in bone marrow. Pol J Radiol 2012:45-50.
5. Cristy M**.** Active bone marrow distribution as a function of age in humans. Phys Med Biol 1981:389-400.
6. Hillengass J, Bauerle T, Bartl R, et al. Diffusion-weighted imaging for non-invasive and quantitative monitoring of bone marrow infiltration in patients with monoclonal plasma cell disease: a comparative study with histology. Br J Haematol 2011:721-8.
7. Schraml C, Schmid M, Gatidis S, et al. Multiparametric analysis of bone marrow in cancer patients using simultaneous PET/MR imaging: Correlation of fat fraction, diffusivity, metabolic activity, and anthropometric data. J Magn Reson Imaging 2015:1048-56.
8. Messiou C, Giles S, Collins DJ, et al. Assessing response of myeloma bone disease with diffusion-weighted MRI. Br J Radiol 2012:e1198-203.
9. Herrmann J, Krstin N, Schoennagel BP, et al. Age-related distribution of vertebral bone-marrow diffusivity. Eur J Radiol 2012:4046-9.

10. Wong AP, Pipitone J, Park MTM, et al. Estimating volumes of the pituitary gland from T1-weighted magnetic-resonance images: effects of age, puberty, testosterone, and estradiol. Neuroimage 2014:216-21.
11. Alhazmi A, Vargas E, Palomo JM, et al. Timing and rate of spheno-occipital synchondrosis closure and its relationship to puberty. PLoS One 2017:e0183305.
12. A LN, L JH, Davis M, et al. The relationships among total body fat, bone mineral content and bone marrow adipose tissue in early-pubertal girls. Bonekey Rep 2013: 2; 315.
13. Izquierdo Ade M, Mishima FD, Carrard VC, et al. Effects of induced precocious puberty on cranial growth in female Wistar rats. Eur J Orthod 2012:133-40.
14. Yingling VR, Khaneja A**.** Short-term delay of puberty causes a transient reduction in bone strength in growing female rats. Bone 2006:67-73.
15. Mahachoklertwattana P, Pootrakul P, Chuansumrit A, et al. Association between bone mineral density and erythropoiesis in Thai children and adolescents with thalassemia syndromes. J Bone Miner Metab 2006:146-52.
16. Wang Q, Nicholson PH, Suuriniemi M, et al. Relationship of sex hormones to bone geometric properties and mineral density in early pubertal girls. J Clin Endocrinol Metab 2004:1698-703.
17. Neubauer H, Evangelista L, Morbach H, et al. Diffusion-weighted MRI of bone marrow oedema, soft tissue oedema and synovitis in paediatric patients: feasibility and initial experience. Pediatr Rheumatol Online J 2012:20.
18. Darge K, Jaramillo D, Siegel MJ**.** Whole-body MRI in children: current status and future applications. Eur J Radiol 2008:289-98.
19. Weber DR, Leonard MB, Zemel BS**.** Body composition analysis in the pediatric population. Pediatr Endocrinol Rev 2012:130-9.

20. Zawin JK, Jaramillo D**.** Conversion of bone marrow in the humerus, sternum, and clavicle: changes with age on MR images. Radiology 1993:159-64.
21. Di Iorgi N, Mo AO, Grimm K, et al. Bone acquisition in healthy young females is reciprocally related to marrow adiposity. J Clin Endocrinol Metab 2010:2977-82.
22. Peng YJ, Yu H, Hao X, et al. Luteinizing hormone signaling restricts hematopoietic stem cell expansion during puberty. Embo j 2018.
23. Gurevitch O, Slavin S, Feldman AG**.** Conversion of red bone marrow into yellow - Cause and mechanisms. Med Hypotheses 2007:531-6.
24. Hayashi K, Kagawa K, Awai M, et al. The role of marrow architecture and stromal cells in the recovery process of aplastic marrow of lethally irradiated rats parabiosed with healthy litter mates. Scan Electron Microsc 1986:1489-99.
25. Le Ster C, Lasbleiz J, Kannengiesser S, et al. A fast method for the quantification of fat fraction and relaxation times: Comparison of five sites of bone marrow. Magn Reson Imaging 2017:157-61.
26. Nonomura Y, Yasumoto M, Yoshimura R, et al. Relationship between bone marrow cellularity and apparent diffusion coefficient. J Magn Reson Imaging 2001:757-60.
27. Li Q, Pan SN, Yin YM, et al. Normal cranial bone marrow MR imaging pattern with age-related ADC value distribution. Eur J Radiol 2011:471-7.
28. Ohno N, Miyati T, Kasai H, et al. Evaluation of perfusion-related and true diffusion in vertebral bone marrow: a preliminary study. Radiol Phys Technol 2015:135-40.
29. Dietrich O, Geith T, Reiser MF, et al. Diffusion imaging of the vertebral bone marrow. NMR Biomed 2017.
30. Messiou C, Collins DJ, Morgan VA, et al. Optimising diffusion weighted MRI for imaging metastatic and myeloma bone disease and assessing reproducibility. Eur Radiol 2011:1713-8.

Tables

Stage		
0	UNFUSED	Completely open with no evidence of fusion between the basilar portion of the occipital and the sphenoid, no bone present in the gap
1	FUSING ENDOCRANIALLY	<50% the length of the synchondrosis is fused proceeding endo- to ectocranially
2	FUSING ECTOCRANIALLY	>50% the length of the synchondrosis is fused, the ectocranial (inferior) border remains unfused
3	COMPLETE FUSION	Completely fused with the appearances of normal bone throughout, a fusion scar may be present.

Table 1 Staging system for pubertal status based on spheno-occipital synchondrosis closure on imaging (adapted from [11]).

	All pre-pubertal N=30	All post pubertal N=30	*p-value (Mann-Whitney U)*
	ADC X10^{-5} mm^2/s Mean ± std		
mean	74.6 ± 18.4	58.2 ± 15.6	0.0001
C25	54.1 ± 16.8	39.9 ± 10.3	0.0001
C50	74.8 ± 18.2	55.7 ± 11.8	0.0001
C75	93.6 ± 24.1	74.0 ± 22.7	0.0002
IQR	39.5 ± 14.2	34.1 ± 17.5	0.2

Table 2 Pre- and post-pubertal mean and centile values of ADC showing significant differences with pubertal status.

	Female pre-pubertal N=15	Female post-pubertal N=15	*p-value (Mann Whitney U)*	Male pre-pubertal N=15	Male post-pubertal N=15	*p-value (Mann Whitney U)*
	ADC X10^{-5} mm^2/s Mean ± std			**ADC X10^{-5} mm^2/s Mean ± std**		
mean	70.7 ± 14.8	58.5 ± 16.3	0.04	78.6 ± 21.3	57.8 ± 15.5	0.005
C25	51.2 ± 11.9	40.2 ± 9.1	0.01	56.9 ± 20.7	39.6 ± 11.7	0.004
C50	69.8 ± 13.7	55.9 ± 10.8	0.009	79.9 ± 21.1	55.6 ± 11.7	0.0002
C75	85.4 ± 16.3	74.2 ± 27.3	0.03	101.7 ± 28.1	73.8 ± 18.0	0.004
IQR	34.2 ± 11.5	34.0 ± 22.0	0.25	44.8 ± 14.9	34.3 ± 11.7	0.06

Table 3 Mean and centile values of ADC pre- and post-puberty by gender, showing that the reductions in ADC post-puberty were present in both females and males.

Figure Legends

Figure 1 Sagittal T1-W midline images through the clivus in a 7-year old female (a) and a 16-year old female (b). In a, the superior aspect of the pituitary is flat (arrowhead) and the synchondrosis unfused (Stage 0, arrowhead). In b, the superior aspect of the pituitary bulges upward (arrowhead) and the synchondrosis is fused (arrow).

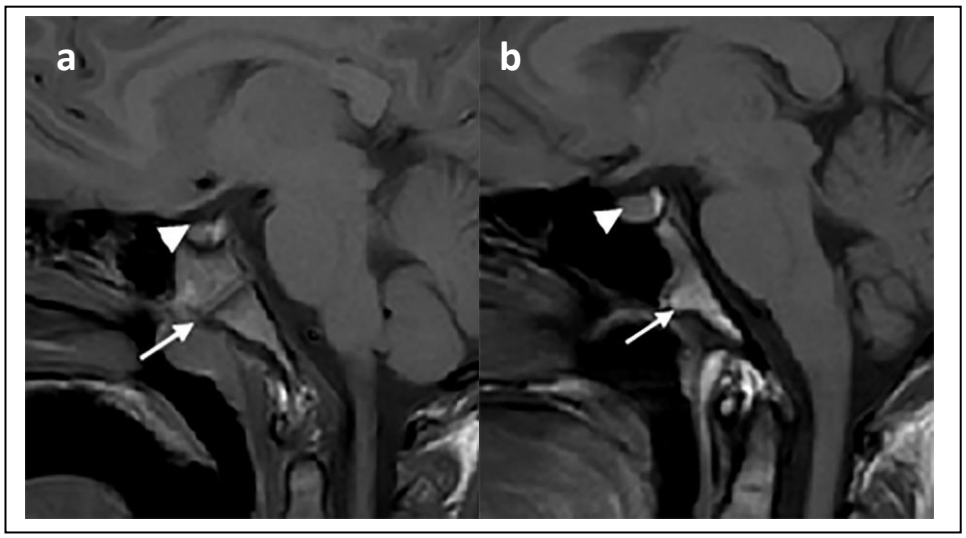

Figure 2 Bland-Altman plots (difference between 2 measurements vs. their mean) showing the variability of the ADC median values (a) and ADC mean values (b) from clivus marrow when derived by 2 independent observers. Data was obtained in a subset of 20 randomly selected patients (5 from each group). All 95% confidence intervals (CI) representing the limits of agreement were less than +/-15%.

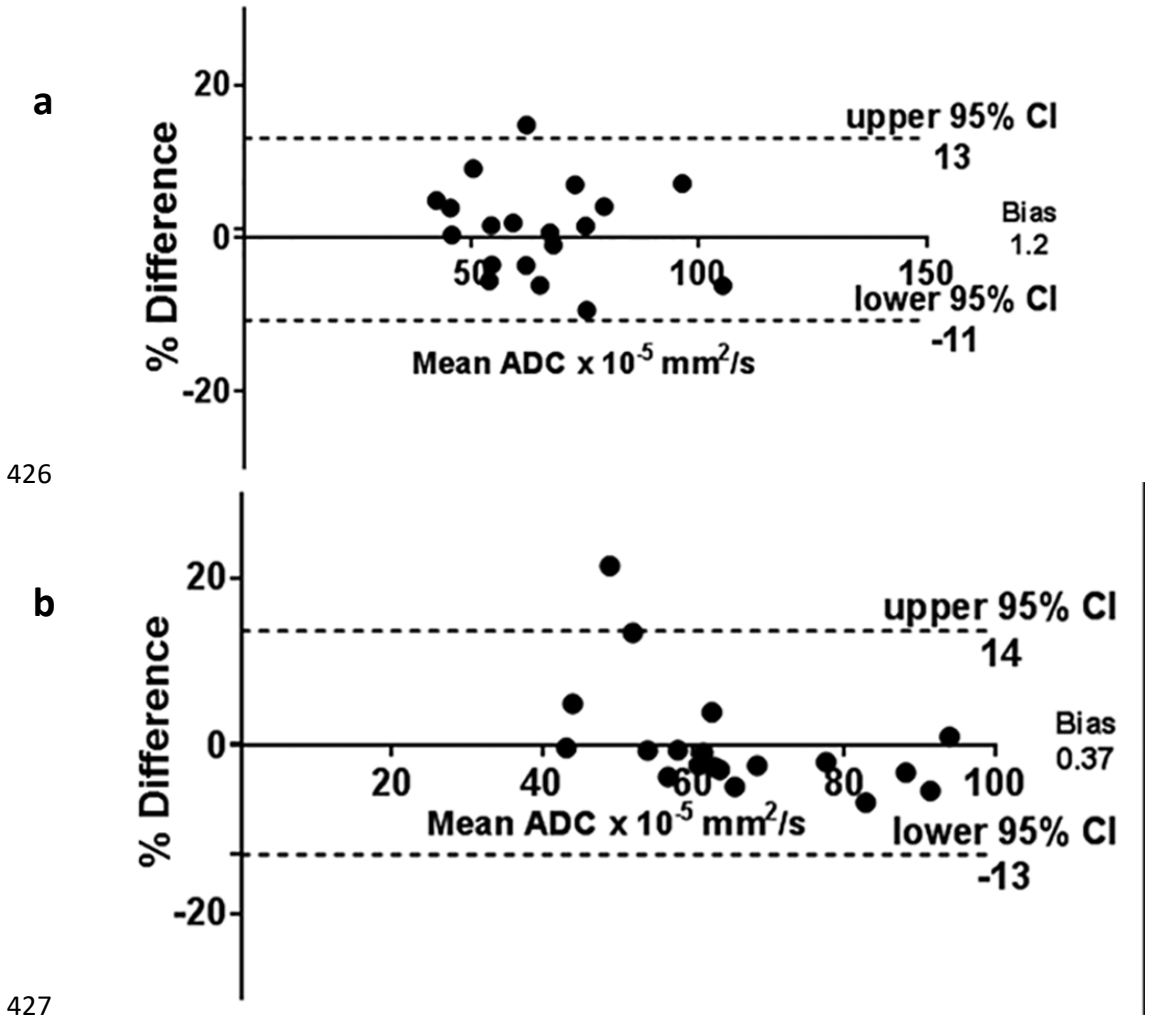

Figure 3 Scatter plots showing the negative correlation of the Apparent Diffusion Coefficient with age in a) whole cohort; b) females alone; c) males alone.

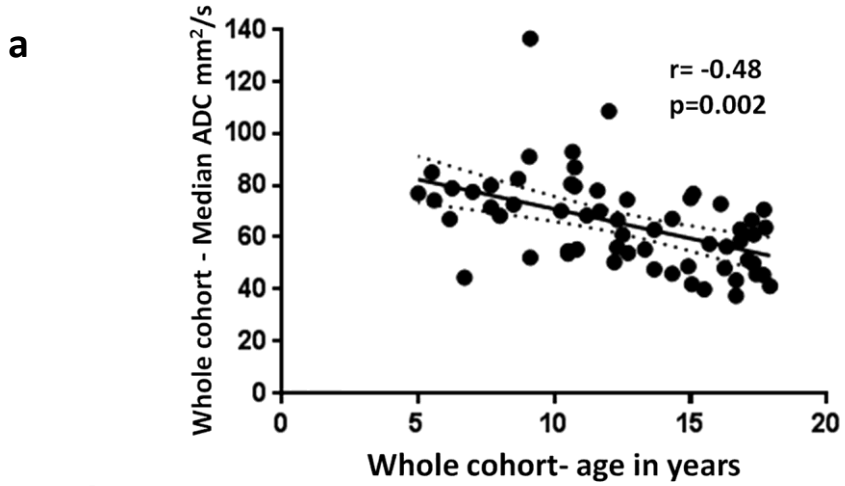

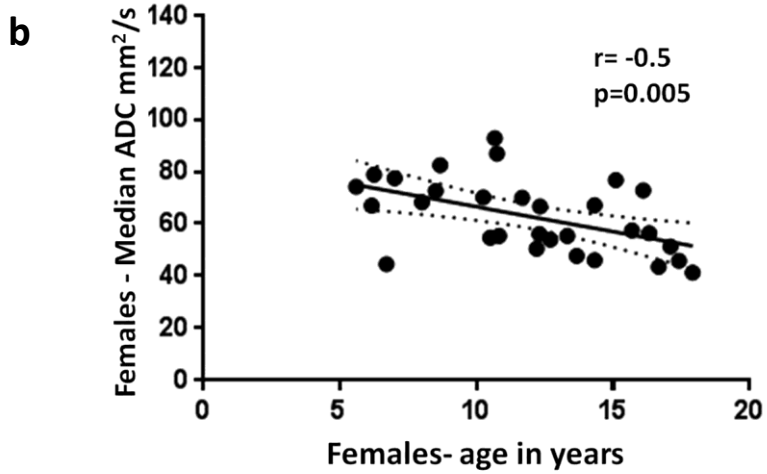

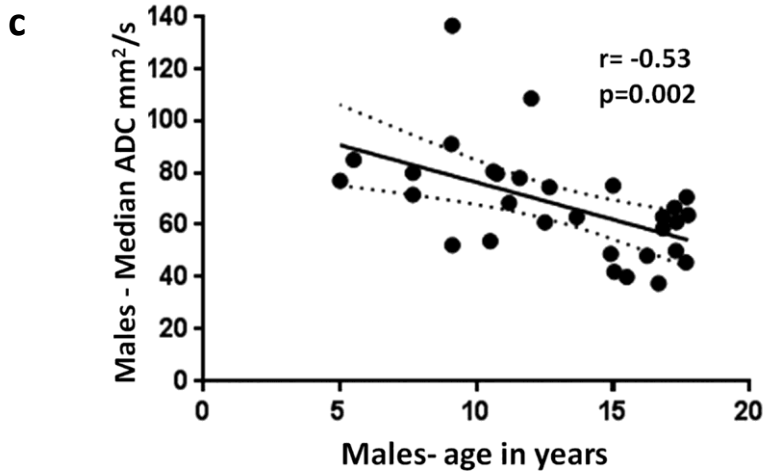

436 **Figure 4** Box and whisker plot comparing ADC between 5-9 year olds, 10 years to puberty
437 and all post-pubertal subjects (a), between pre- and post-pubertal females (b) and pre- and
438 post-pubertal males (c).

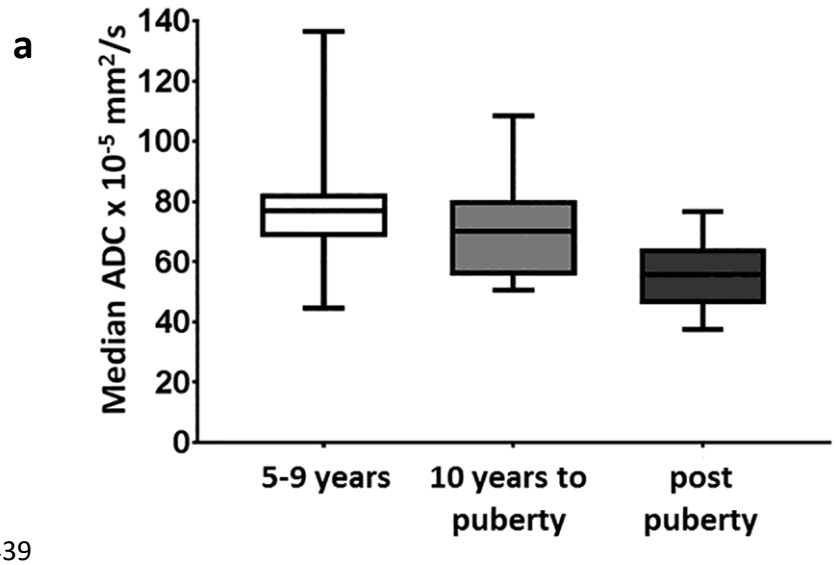

439

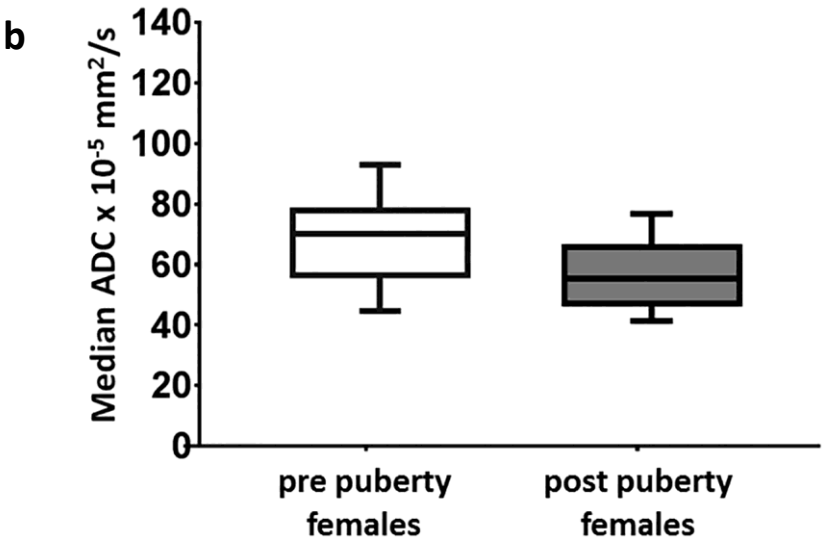

440

c

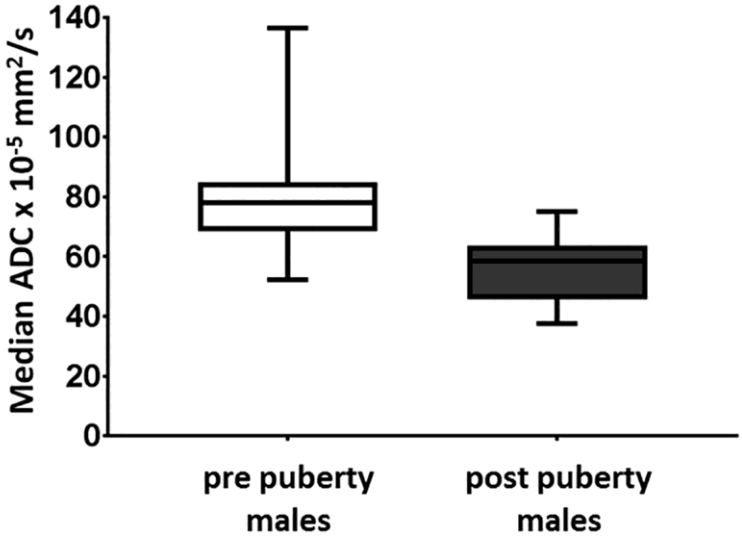
Median ADC x 10-5 mm2/s
140
120
100
80
60
40
20
0
pre puberty males
post puberty males

441

442

443

444 **Figure 5** Histogram plots for the whole population pre- and post-puberty (a) and for post-
445 pubertal females alone vs. all pre-pubertal subjects (b) and males alone vs. all pre-pubertal
446 subjects (c). There is a left shift in the histograms post-puberty, regardless of gender.

447

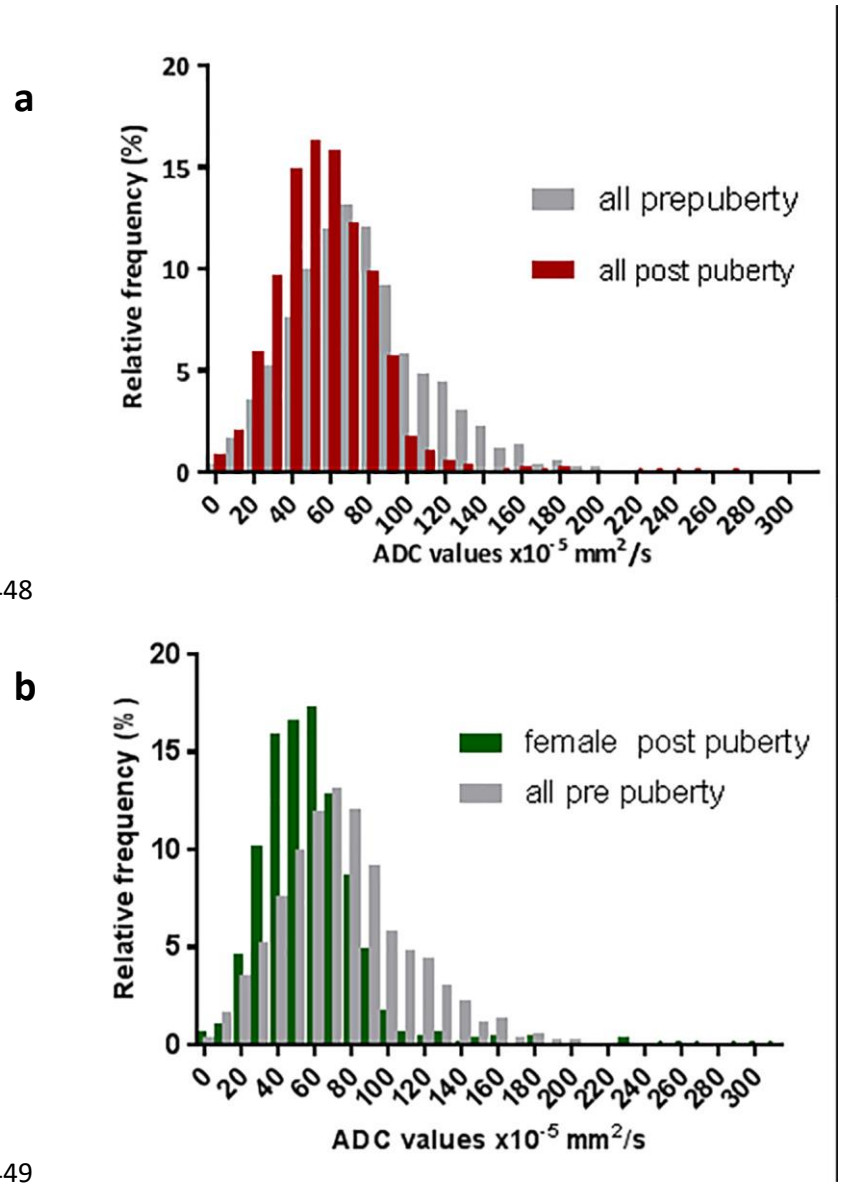

448

449

c

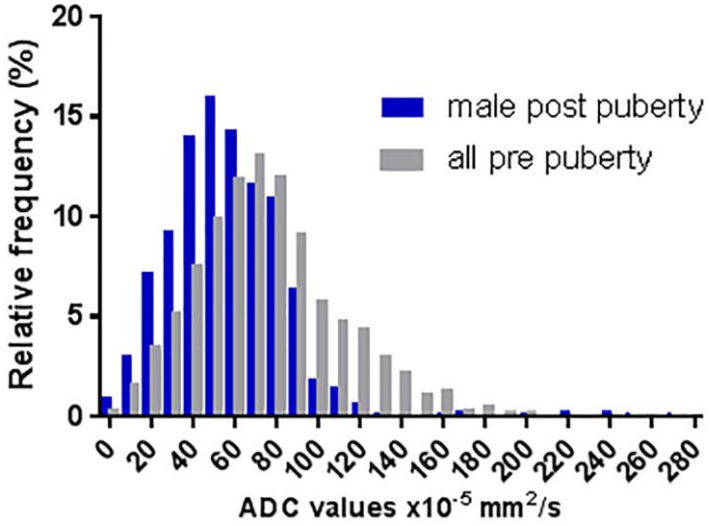
Relative frequency (%)
20
15
10
5
0
male post puberty
all pre puberty
0
20
40
60
80
100
120
140
160
180
200
220
240
260
280
ADC values x10-5 mm2/s

450

Figure 6 Axial T2-W (a), Diffusion weighted (b) and ADC map (c) in a 5.5 year-old pre-pubertal male. Intermediate signal-intensity within the marrow of the clivus is noted in (a) with corresponding high signal intensity in (b). ADC of the hypercellular marrow in (c) is 84.0 ± 22.2 mm^2/s.

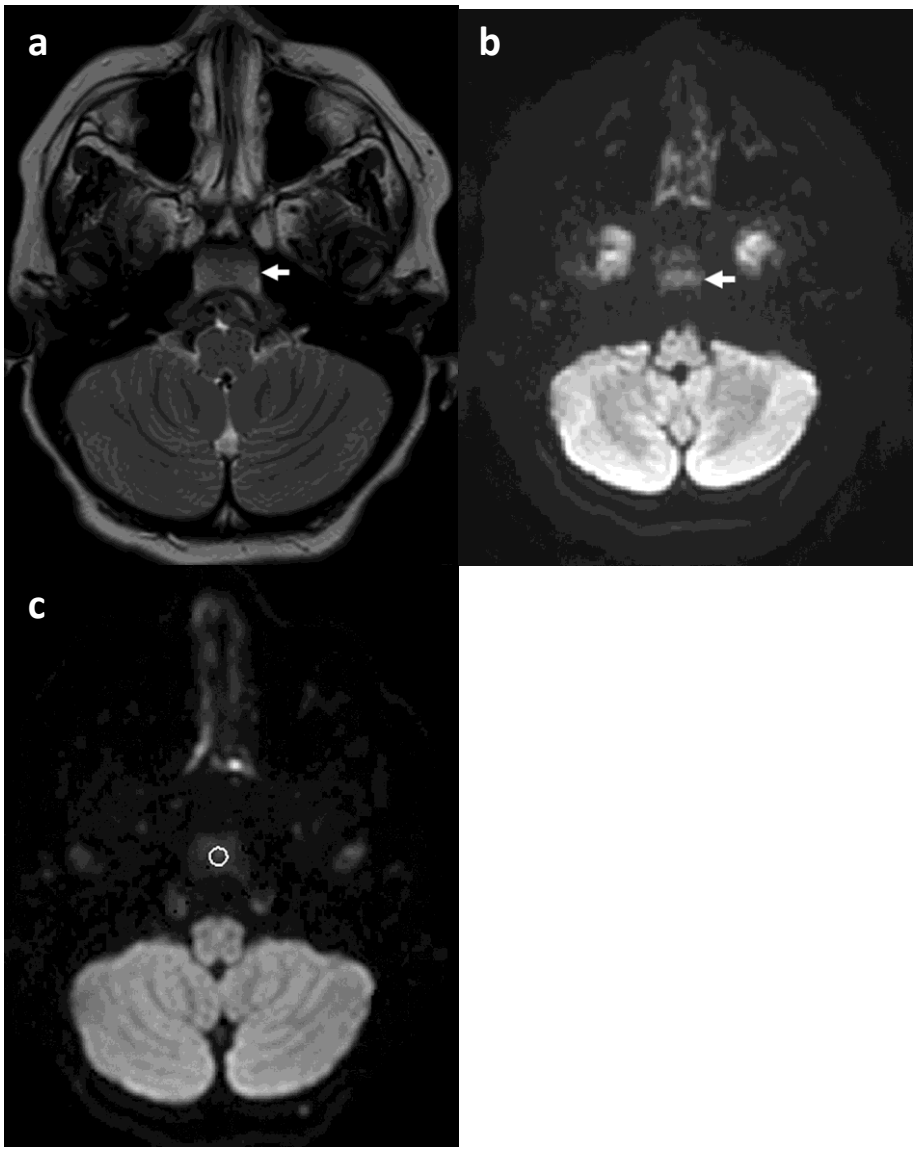

Figure 7 Axial T2-W (a), Diffusion weighted (b) and ADC map (c) in a 16.8 year-old post-pubertal male. High signal equivalent to that of fat is noted in the marrow of the clivus in (a) with corresponding low signal intensity on the fat-suppressed diffusion-weighted image in (b). Low ADC (38.4 ± 15.9 mm^2/s) of the fat replaced marrow is evident in (c).